Proceedings of the 7th World Congress on Recent Advances in Nanotechnology (RAN'22)
~~Lisbon, Portugal~~ Virtual Conference – April 04 – 06, 2022
Paper No. ICNNFC 162
DOI: 10.11159/icnnfc22.162

Development of Room-temperature H_2S Gas Sensor Using Flower-like ZnO Nanorods

Sara Ghaderahmadi [1], Nishat Tasnim [1], Mohammad Arjmand [2], Mina Hoorfar [1]

[1] Faculty of Engineering and Computer Science, University of Victoria, Victoria, Canada
[2] School of Engineering, University of British Columbia, Okanagan Campus, Kelowna, Canada

Abstract **-** Flower-like ZnO nanorods have been directly deposited on a glass substrate with prefabricated interdigitated electrodes using a modified hydrothermal method. The flower-like nanorods were fabricated in two different rod dimensions and grain sizes. X-ray diffraction (XRD), X-ray photoelectron spectroscopy (XPS), and scanning electron microscopy (SEM) characterization measurements were performed to confirm the uniform hexagonal wurtzite structure of the ZnO nanorods. The H_2S gas sensing properties of the nanorod samples were investigated at room temperature. The response value of 7.4 with 293s response time and 186s recovery time is achieved toward 100ppm H_2S at room temperature, demonstrating the potential of the sensing layer as a promising candidate for room temperature gas sensing applications.

Keywords**:** H_2S, nanomaterials, nanorods, ZnO

1. Introduction

Hydrogen sulfide (H_2S) is a highly flammable and toxic gas. Also known as sewer gas, this hazardous gas can be produced as a by-product of various industrial processes such as petroleum and natural gas extraction and purification, paper and pulp manufacturing, textile production, chemical manufacturing, wastewater treatment, and food processing (Habeeb, Kanthasamy et al. 2018). H_2S gas is heavier than air and can be collected in low-lying and enclosed areas at or below ground level, making these confined spaces hazardous for work (Rubright, Pearce et al. 2017). Common health hazards from exposure include nausea, skin and eye irritation, headache, unconsciousness, and in some severe cases even death. Therefore, H_2S gas sensors are a significantly important component in environmental and industrial applications. As a result, various efforts have been made to develop an efficient H_2S gas sensor.

Among the different mechanisms employed to detect H_2S (Li, Zu et al. 2019, Zhang, Wang et al. 2019, Ghaderahmadi, Kamkar et al. 2021), metal oxide semiconductors (MOS) have been reported to be the most promising candidate due to their low cost, ease of fabrication, and high thermal and mechanical stability (Zhu and Zeng 2017, Agarwal, Rai et al. 2019). MOS-based sensing layers can operate in a wide range of temperatures in different geometries from bulk to nanostructures. MOS-based gas sensors usually operate at high operating temperatures (i.e., >150℃) (Ghazi, Janfaza et al. 2021, Pravarthana, Tyagi et al. 2021). The elevated operating temperature has some major drawbacks including increased power consumption and decreased long-term stability (Li, Tang et al. 2019, Shewale and Yun 2020). Moreover, there can be explosion hazards in the existence of explosive gases such as H_2S.

To date, only a few metal oxides have been employed for H_2S gas sensing at reduced operating temperatures, and, among all, ZnO is reported to provide the most promising characteristics for room temperature H_2S gas sensing, both in terms of high response value and fast response and recovery kinetics (Ghaderahmadi, Kamkar et al. 2021). In this study, we have fabricated flower-like ZnO nanorods and investigated their potential for room temperature gas sensing. The samples are fabricated in two different grain sizes (19 and 23nm) using a modified hydrothermal method. The gas sensing properties of the samples (i.e., response value, response time, and recovery time) are investigated at room temperature. We also elucidated the effect of the ZnO nanorods grain size on its gas sensing properties.

2. Materials and Methods

2.1. Synthesis of flower-like ZnO nanorods

Two different morphologies of ZnO nanostructures were directly grown on a glass substrate using a modified hydrothermal method (Shi, Yang et al. 2013). The glass substrates with prefabricated interdigitated electrodes were washed

with acetone and sonicated in deionized water/ethanol and dried with N_2. 0.5g of $ZnO.6H_2O$ was dissolved in two different ratios of ethanol and deionized water, stirred for 10min at room temperature to form a 40 ml solution. Next, 2ml NH_4OH was added dropwise into the as-prepared solution and then stirred for 1hr at room temperature. Finally, the glass substrate with prefabricated IDEs was immersed into the precursor solution and sealed in a stainless-steel autoclave for 24hr at 70℃. After the 24hr, the flower-like ZnO nanorods were directly deposited on the glass substrate, and finally, they were annealed for 1hr at 90℃ to form the final sensing layer. Samples with 20/20 ethanol/water and 10/30 ethanol/water were named S1 and S2, respectively.

2.2. Response analysis

To investigate the gas sensing properties of the in-situ deposited flower-like ZnO nanorods (i.e., samples S1 and S2) at room temperature, the gas sensor was placed in a 40-liter gas testing chamber and exposed to different gas concentrations and connected to an external measurement setup. The changes in the sensing layer resistance upon exposure to different concentrations of different analytes are monitored using Potentistat (VERSASTAT 4) and it is used to investigate its gas sensing properties (i.e., response value, response time, recovery time, selectivity, and long/short-term stability). The gas sensor is characterized based on six criteria: response value, response time, recovery time, selectivity, stability, and reproducibility. The response value is defined as the ratio of the sensor resistance in steady-state in ambient air over the sensor resistance upon exposure to a reducing target gas ($^{R_a}/_{R_g}$). The response time and recovery time are defined as the time for the sensor to reach 90% of the total change upon exposure to the target gas and ambient air, respectively. Selectivity is defined as the ability of the sensor to distinguish between different response signals obtained toward different analytes. To investigate the selectivity of the samples, the sensing layers were exposed to 100ppm of H_2S, N_2O, ethanol, isopropanol, 2-pentanol, and toluene and the response values were compared. To obtain the desired concentrations of ethanol, isopropanol, 2-pentanol, and toluene, certain amounts of each analyte was directly injected into the gas chamber. The microheater in the gas chamber evaporates the target analyte and the fan homogenises the air in the gas chamber. To obtain the desired concentrations of the gas analytes (i.e., H_2S and N_2O), the gas flow rate was controlled using a mass flow controller and was directly injected into the gas chamber and fan homogenised the air in the gas chamber.

3. Results and Discussion

3.1. Material characterization

The crystallinity of the ZnO nanorods was investigated using X-Ray diffraction (XRD) as shown in Figure 2a. The diffraction patterns are well indexed to hexagonal wurtzite ZnO crystalline structure with JCPDS card no. 01-079-0205 (Yin, Liu et al. 2014, Gao, Cheng et al. 2019). The sharp and strong peak at 36.5° indicates high crystallinity in both samples. However, the peaks are slightly sharper in the S2 sample, implying higher crystallinity in the sample with less ethanol in the precursor solution. Moreover, no other characteristic peaks were observed in the XRD spectra, showing that the crystalline ZnO nanorods were synthesized with high purity and uniformity. According to the Scherrer equation and based on the data extracted from the XRD patterns, the average grain size of samples S1 and S2 were found to be 23 and 19nm, respectively.

The chemical composition of the sample S2 was investigated using X-ray photoelectron spectroscopy (XPS). As it can be seen in Figure 2b, except for a carbon peak (C1s), the full spectra confirmed the high chemical purity of the nanorods consisting of only Zn and O. Figure 2c, shows the Gaussian fitting curves of the O1s spectra of the ZnO nanorods. The peak at 532eV is attributed to the O_2^- ions within the ZnO matrix. Figure 2d shows the magnified XPS spectra of the ZnO nanorods with two peaks at 1022.1 and 1045.3, attributed to $Zn2p_{2/3}$ and $Zn2p_{1/2}$. The observed values are in good agreement with the literature, confirming a ZnO hexagonal wurtzite structure (Shaikh, Ganbavale et al. 2018).

Fig. 1 shows the SEM images of flower-like ZnO nanorods. The hexagonal structure of the ZnO nanorods could be directly observed from the top view SEM images. The uniformity of both samples can be confirmed from SEM images in Fig. 1a, d. Moreover, comparing the images from samples S1 and S2, the rods in sample S2, are narrower and longer compared to their other counterpart, which can be attributed to the increased kinetics of synthesis reaction due to the lower amount of ethanol in the precursor solution.

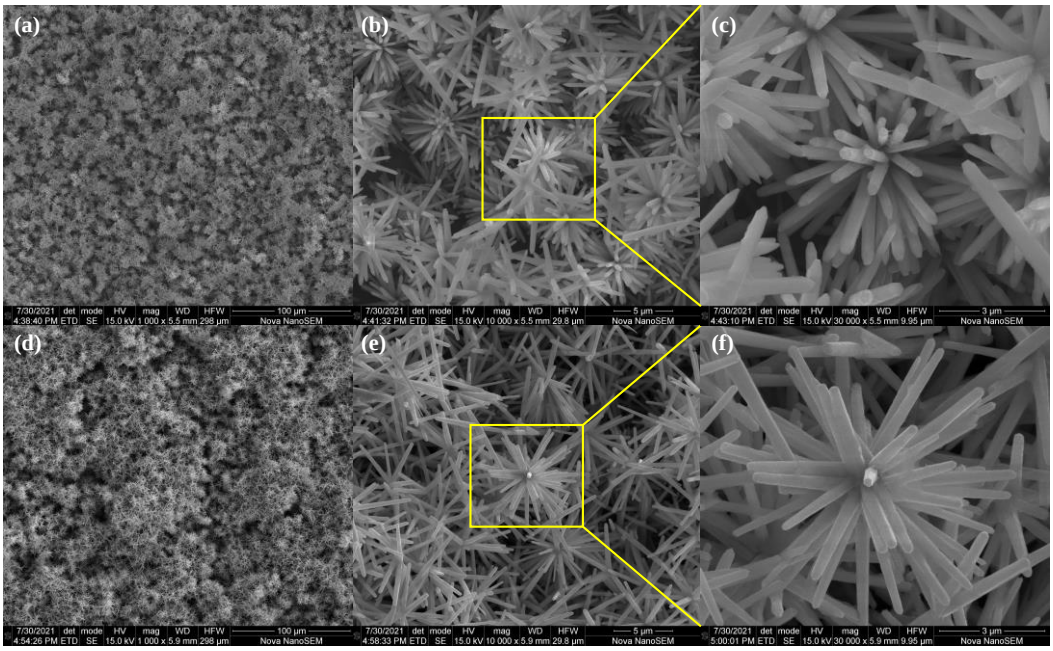

Fig. 1. (a, b, c) and (d, e, f) SEM images of samples S1and S2 at different magnifications.

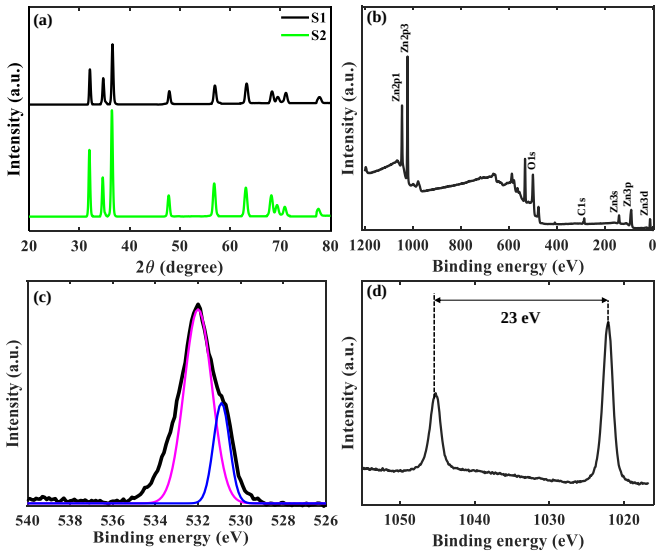

Figure 2 (a) XRD spectra of the samples S1 and S2, XPS spectrum of the ZnO sample S2 (a) full spectrum, (b) O spectrum, and c) Zn spectrum.

3.2. H_2S gas sensing properties

The sensing properties of samples S1 and S2 was investigated toward H_2S at room temperature. As presented in Figure 3a, the response as a function of gas concentration showed a linear increasing trend with higher response values obtained from sample S2. Based on the measured values, the sensitivity of samples S1 and S2 were 1.213 and 1.932, respectively. Figure 3b, c shows the dynamic response of the samples S1 and S2 upon exposure to 100ppm H_2S. The response value of S1 and S2 was measured 5.4 and 7.4, respectively. The results showed that despite the higher response value of sample S2, the response at recovery kinetics were faster for sample S1, e.g., 206 and 126s for sample S1 and 293 and 186s for sample

S2 as response time and recovery time, respectively. The higher response value of sample S2 is attributed to the smaller grain size compared to sample S1. The smaller grain size of the sample S2 results in a higher ratio of depletion layer width over the conduction bandwidth. Moreover, the lower response and recovery time of sample S1 is attributed to the lower response value compared to sample S2. The promising sensing properties of sample S2 at room temperature can be attributed to a large surface area provided by the lengthy nanorods, as well as the enhanced connections between the rods, due to its the flower-like structure.

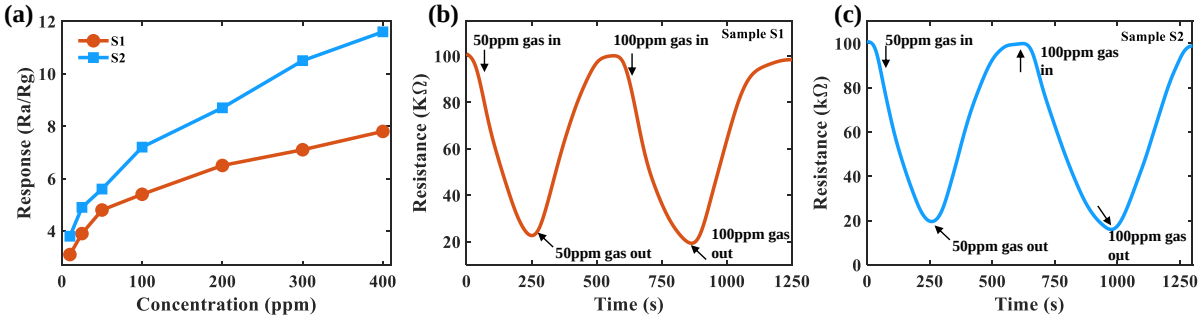

Figure 3 (a) The response value as a function of H_2S concentration for samples S1 and S2. The dynamic response of samples (b) S1 and (c) S2 toward 50 and 100ppm H_2S.

Samples S1 and S2 were exposed to a range of interfering gases in different concentration ranging from 50 to 400ppm to investigate their selectivity toward H_2S. Investigating the response values, the of response value toward H_2S was in average 65.72% and 69.19% higher compared with the interfering gases in samples S1 and S2, respectively. The results imply high selectivity of samples toward H_2S. The high selectivity of both samples towards H_2Scan be attributed to three phenomena. First, the bond energy of H-HS in H_2S is lower compared with other interfering gases; thus, it can be easily decomposed at room temperature (Ramgir, Sharma et al. 2013, Hosseini and Mortezaali 2015). Second, H_2S is a strong reducing gas, therefore the interaction strength between ZnO and H_2S is higher compared to the other interfering gases. Third, unlike the other interfering gases, the reaction between ZnO and H_2S (which is also called desulfurization reaction) is exothermic. Therefore, the desulfurization reaction can happen simultaneously with the reaction between the adsorbed oxygen species and adsorbed H_2S. This spontaneous reaction results in a higher sensitivity toward H_2S (Liu, Fan et al. 2009).

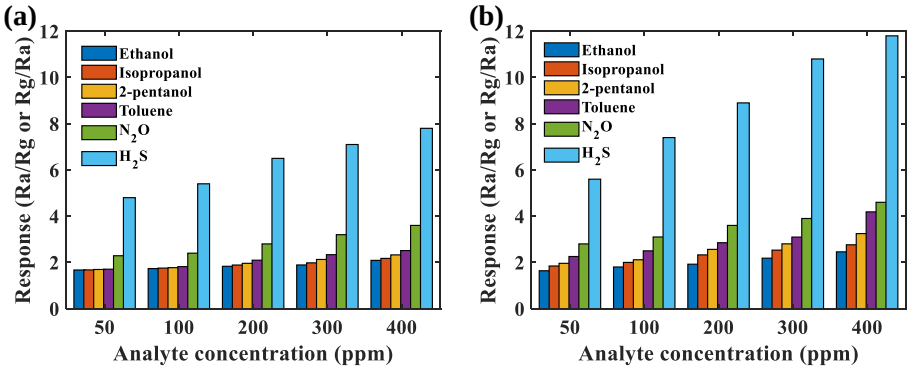

Figure 4 The response value of samples (a) S1 and (b) S2 toward different interfering gases at room temperature.

3.3. Gas sensing mechanism

The sensing mechanism of MOS is based on conductivity change upon exposure to a target gas. At the steady-state condition, oxygen is adsorbed at the metal-oxide surface in the form of O_2^- at room temperature (Agarwal, Rai et al. 2019), creating an electron depletion layer on the surface of an n-type semi-conductor (a type of semiconductor in which the majority of charge carriers are electrons) (Zang, Nie et al. 2014). Upon exposure to a reducing target gas, the adsorbed oxygen species

react with the target gas, decreasing the width of the depletion layer, and therefore, the sensor increasing the electrical conductivity (Ugale, Umarji et al. 2020).

Investigating the response values toward samples S1 and S2, it becomes clear that the response value toward sample S2 is higher compared with sample S1. This can be attributed to two main parameters: surface area and grain size. As it can be concluded from the SEM images of samples S1 and S2, the longer and narrower geometry of ZnO nanorods in sample S2 provides a higher surface area compared with sample S1. The higher surface area provides more active sites at the surface of the metal oxide to adsorb oxygen and react with the target gas. Therefore, the response value of sample S2 is higher than sample S1.

Another important parameter that has affected the response value difference between the samples is the average grain size. In a crystalline structure, if the average grain size is smaller than the Debye length (λ_D), the conduction band becomes fully depleted. In this case, the metal oxide is highly sensitive, and the sensing properties highly depend on the rod diameter (Li, Du et al. 2007). On the other hand, if the grain size is significantly larger than the Debye length, the conduction band becomes partly depleted (Korotcenkov 2008), the sensing properties are mostly determined by the junction between the nanorods. The barrier at these junctions is only affected by the type of the target gas and its concentration. Therefore in partly depleted nanostructures the surface interactions have a less significant effect on the entire layer's conductivity (Walker, Akbar et al. 2019). In other words, in partly depleted sensing layers, the response resistance value is directly affected by the ratio of the width of the depletion layer over the width of the conduction band (Korotcenkov 2008). In this study, according to the XRD results, the average grain size of samples S1 and S2 have calculated 23 and 19nm, respectively. This means both sensing layers are partly depleted at the steady-state (Korotcenkov 2008, Nundy, Eom et al. 2020). Because sample S2 provides a higher width ratio of the depletion layer over the conduction band due to its smaller grain size, the response value of sample S2 was greater compared to sample S1.

4. Conclusion

A modified hydrothermal method was employed to fabricate flower-like ZnO nanostructure in two different rod dimensions and grain sizes. The grain size was controlled by the ratio of water/ethanol in the precursor solution. Investigating the crystallinity of the samples using XRD, XPS, and SEM showed samples are fabricated with 19 and 23nm grain size (named as S2 and S1, respectively) in a uniform hexagonal wurtzite structure of the ZnO nanorods. The H_2S gas sensing properties of the samples were investigated at room temperature. The response value of 5.4 and 7.4, was obtained from the samples S1 and S2, respectively, toward 100ppm H_2S. The response/recovery times were measured at 206/126s and 293/186s for samples S1 and S2, respectively. These promising gas sensing features of the flower-like ZnO nanorods-based sensing layer can be exploited for the development of room-temperature gas sensing devices for health and safety monitoring applications.

References

[1] Agarwal, S., P. Rai, E. N. Gatell, E. Llobet, F. Güell, M. Kumar and K. Awasthi (2019). "Gas sensing properties of ZnO nanostructures (flowers/rods) synthesized by hydrothermal method." Sensors and Actuators B: Chemical **292**: 24-31.

[2] Gao, R., X. Cheng, S. Gao, X. Zhang, Y. Xu, H. Zhao and L. Huo (2019). "Highly selective detection of saturated vapors of abused drugs by ZnO nanorod bundles gas sensor." Applied Surface Science **485**: 266-273.

[3] Ghaderahmadi, S., M. Kamkar, N. Tasnim, M. Arjmand and M. Hoorfar (2021). "A review of low-temperature H 2 S gas sensors: fabrication and mechanism." New Journal of Chemistry.

[4] Ghazi, M., S. Janfaza, H. Tahmooressi, A. Ravishankara, E. Earl, N. Tasnim and M. Hoorfar (2021). "Enhanced selectivity of microfluidic gas sensors by modifying microchannel geometry and surface chemistry with graphene quantum dots." Sensors and Actuators B: Chemical **342**: 130050.

[5] Habeeb, O. A., R. Kanthasamy, G. A. Ali, S. Sethupathi and R. B. M. Yunus (2018). "Hydrogen sulfide emission sources, regulations, and removal techniques: a review." Reviews in Chemical Engineering **34**(6): 837-854.
[6] Hosseini, Z. and A. Mortezaali (2015). "Room temperature H2S gas sensor based on rather aligned ZnO nanorods with flower-like structures." Sensors and Actuators B: Chemical **207**: 865-871.
[7] Korotcenkov, G. (2008). "The role of morphology and crystallographic structure of metal oxides in response of conductometric-type gas sensors." Materials Science and Engineering: R: Reports **61**(1-6): 1-39.
[8] Li, C., Z. Du, L. Li, H. Yu, Q. Wan and T. Wang (2007). "Surface-depletion controlled gas sensing of ZnO nanorods grown at room temperature." Applied Physics Letters **91**(3): 032101.
[9] Li, D., Y. Tang, D. Ao, X. Xiang, S. Wang and X. Zu (2019). "Ultra-highly sensitive and selective H2S gas sensor based on CuO with sub-ppb detection limit." International Journal of Hydrogen Energy **44**(7): 3985-3992.
[10] Li, D., X. Zu, D. Ao, Q. Tang, Y. Fu, Y. Guo, K. Bilawal, M. B. Faheem, L. Li and S. Li (2019). "High humidity enhanced surface acoustic wave (SAW) H2S sensors based on sol–gel CuO films." Sensors and Actuators B: Chemical **294**: 55-61.
[11] Liu, Z., T. Fan, D. Zhang, X. Gong and J. Xu (2009). "Hierarchically porous ZnO with high sensitivity and selectivity to H2S derived from biotemplates." Sensors and Actuators B: Chemical **136**(2): 499-509.
[12] Nundy, S., T.-y. Eom, K.-Y. Song, J.-S. Park and H.-J. Lee (2020). "Hydrothermal synthesis of mesoporous ZnO microspheres as NOX gas sensor materials—Calcination effects on microstructure and sensing performance." Ceramics International **46**(11): 19354-19364.
[13] Pravarthana, D., A. Tyagi, T. Jagadale, W. Prellier and D. Aswal (2021). "Highly sensitive and selective H2S gas sensor based on TiO2 thin films." Applied Surface Science **549**: 149281.
[14] Ramgir, N. S., P. K. Sharma, N. Datta, M. Kaur, A. Debnath, D. Aswal and S. Gupta (2013). "Room temperature H2S sensor based on Au modified ZnO nanowires." Sensors and Actuators B: Chemical **186**: 718-726.
[15] Rubright, S. L. M., L. L. Pearce and J. Peterson (2017). "Environmental toxicology of hydrogen sulfide." Nitric oxide: biology and chemistry **71**: 1.
[16] Shaikh, S., V. Ganbavale, S. Mohite, U. Patil and K. Rajpure (2018). "ZnO nanorod based highly selective visible blind ultra-violet photodetector and highly sensitive NO2 gas sensor." Superlattices and Microstructures **120**: 170-186.
[17] Shewale, P. S. and K.-S. Yun (2020). "Synthesis and characterization of Cu-doped ZnO/RGO nanocomposites for room-temperature H2S gas sensor." Journal of Alloys and Compounds **837**: 155527.
[18] Shi, R., P. Yang, X. Dong, Q. Ma and A. Zhang (2013). "Growth of flower-like ZnO on ZnO nanorod arrays created on zinc substrate through low-temperature hydrothermal synthesis." Applied Surface Science **264**: 162-170.
[19] Ugale, A. D., G. G. Umarji, S. H. Jung, N. G. Deshpande, W. Lee, H. K. Cho and J. B. Yoo (2020). "ZnO decorated flexible and strong graphene fibers for sensing NO2 and H2S at room temperature." Sensors and Actuators B: Chemical **308**: 127690.
[20] Walker, J. M., S. A. Akbar and P. A. Morris (2019). "Synergistic effects in gas sensing semiconducting oxide nano-heterostructures: A review." Sensors and Actuators B: Chemical **286**: 624-640.
[21] Yin, M., M. Liu and S. Liu (2014). "Diameter regulated ZnO nanorod synthesis and its application in gas sensor optimization." Journal of alloys and compounds **586**: 436-440.

[22] Zang, W., Y. Nie, D. Zhu, P. Deng, L. Xing and X. Xue (2014). "Core–shell In2O3/ZnO nanoarray nanogenerator as a self-powered active gas sensor with high H2S sensitivity and selectivity at room temperature." The Journal of Physical Chemistry C **118**(17): 9209-9216.
[23] Zhang, Y., Y. Wang, Y. Liu, X. Dong, H. Xia, Z. Zhang and J. Li (2019). "Optical H2S and SO2 sensor based on chemical conversion and partition differential optical absorption spectroscopy." Spectrochimica Acta Part A: Molecular and Biomolecular Spectroscopy **210**: 120-125.
[24] Zhu, L. and W. Zeng (2017). "Room-temperature gas sensing of ZnO-based gas sensor: A review." Sensors and Actuators A: Physical **267**: 242-261.